Special issue of the 3rd International Conference on Computational and Experimental Science and Engineering (ICCESEN 2016)

Prevailing Parameter Evaluation with Heat Transfer Analysis of Absorber Plate in the Flat Solar Collector

Z. Er*

Istanbul Technical University, Faculty of Science and Letters, Physics Engineering Department (13b), 34469 Maslak-Istanbul, Turkey

Solar radiation coming to a solar panel is absorbed and converted into thermal energy, increasing its temperature. This study is focused on the solar thermal panels. As known, the analysis of thermal performance of the collector includes such parameters as solar irradiance, ambient temperature and configuration of collectors etc. In this study, thermal analysis of the absorbent plate of a flat plate solar collector and the temperature transfer to the working fluid, were investigated. During thermal analysis the absorbent plate was considered as an one-dimensional fin. It is assumed that lower surface of the solar panel is ideally insulated in this study. Therefore solar irradiance and heat loss to the environment are analyzed at the upper surface of the absorber plate. This study is aimed to investigate the relations of temperature distribution on the absorber plate and heat transfer from the absorber plate to the fluid. The achievable maximum fluid temperature at the practical working conditions, which quantifies the availability of usable heat energy, obtained by the collector, has been determined as a function of solar irradiance. Procedure is based on steady state analysis and on calculation of the thermal performance of flat-plate collector. The effects of the parameters, which determine the collector efficiency, have been investigated by evaluating all results. Results show that the flat-plate collector performs good and provides the desired quantity of hot water.

DOI: 10.12693/APhysPolA.132.1025

PACS/topics: 88.40.–J, 44.40.+A, 44.25.+F, 44.05.E

1. Introduction

Technological advancements are constantly being made in the solar power industry. Several studies in the world discuss aspects of thermal or photovoltaic systems, designed to produce both the hot fluid, such as water, and the electricity. The Sun emits energy in the form of electromagnetic waves (radiation). Solar radiation is the radiant energy emitted from the Sun. Solar radiation striking an object is absorbed, transmitted or reflected.

The power or instantaneous rate of energy, originated from the Sun and received by a surface is called solar irradiance. In other words, solar irradiance is the amount of solar radiation received per unit area of a given surface.

Solar insolation refers to quantity of solar radiation energy received by a surface of given size during an amount of time. In practice, the irradiance is commonly measured by the average rate of accumulation of energy over one hour, for each hour of the day (kW/m^2) or, taking into account the time factor, kWh/(kWp year). The irradiance essentially denotes the instantaneous rate in which power is delivered to a surface, while the insolation denotes the cumulative sum, total amount of the energy, striking the surface for a specified time interval. This interval must be specified in order to make sense, and the typical unit of time measurement is the hour, as mentioned above. Consequently, irradiance equals to power per unit area and insolation equals to power multiplied by time per area.

The incident solar energy is partially absorbed by a dark and opaque surface, part of this energy is transferred to the fluid in solar thermal collectors [1]. Solar thermal collectors are classified as shown in Table I, according to their thermal operation output, as low, medium, or high-temperature collectors [2].

TABLE I

Collector types and working temperatures for solar thermal systems.

Collector types for solar thermal systems	
Low temp. $\approx 35\,^{\circ}$C	• Not-covered with polymer absorber • These are generally used to heat swimming pools. Operate at high efficiency levels when temperature difference is between 5 and 30 °C (41 and 86° F)
Medium temp. $\approx 80\,^{\circ}$C	• Transparent covered collectors • These are also usually flat plates, but are used for heating water or air for residential and commercial use. Operate when temperature difference is between 15 and 200 °C (59 and 392° F)
High temp. $\approx 120\,^{\circ}$C	• Advanced covered collectors • High-temperature collectors concentrate sunlight using mirrors or lenses and are generally used for fulfilling heat requirements up to 300 °C/20 bar pressure in industries, and for electric power production
Process heat temp. $\geq 200\,^{\circ}$C	Advanced covered collectors

*e-mail: erzuh@itu.edu.tr

The most common solar collectors for solar water-heating systems are made in form of flat-plate collectors and vacuum tube collectors. This study will be focused on flat-plate collectors. A typical flat-plate collector is a box insulated by a casing, with a transparent cover, such as glass or plastic cover (called glazing), thermal insulation material, an absorber plate and tubes, as illustrated in Fig. 1 [3].

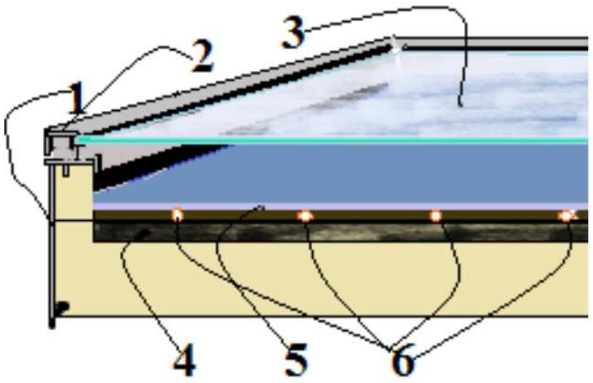

Fig. 1. Flat plate collector construction. 1–Casing, 2–Seal, 3–Transparent cover, 4–Thermal insulation, 5–Absorber plate, 6–Tube.

2. Thermal analysis for absorber plate

Several factors affect the efficiency value of conversion of a thermal system, which include its thermodynamic efficiency, optic efficiency, such as reflectance efficiency, and conduction efficiency. The schematic diagram of efficiency/performance factors for a flat-plate collector is illustrated in Fig. 2.

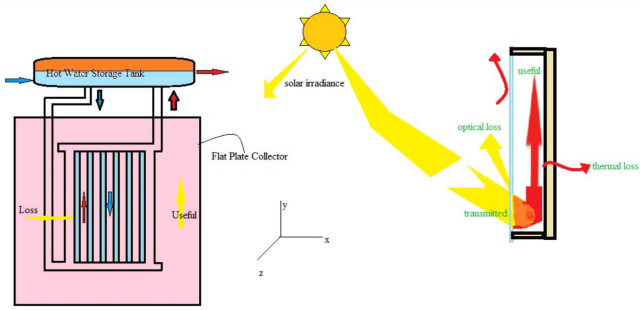

Fig. 2. Schematic diagram of a flat plate collector.

There are various relations that are required in order to determine the collected useful energy and the influence of various constructional parameters on the performance of a collector. Figure 3 shows the outline of a flat-plate collector for water heating and the main parameters involved in heat transfers: incident solar radiation G, cover heat loss, convective heat transfer between cover and air, convective heat transfer between plate and fluid, radiation heat transfer between plate and cover [4, 5]. Figure 4 shows heat transfer and resistance network for the flat-plate collector.

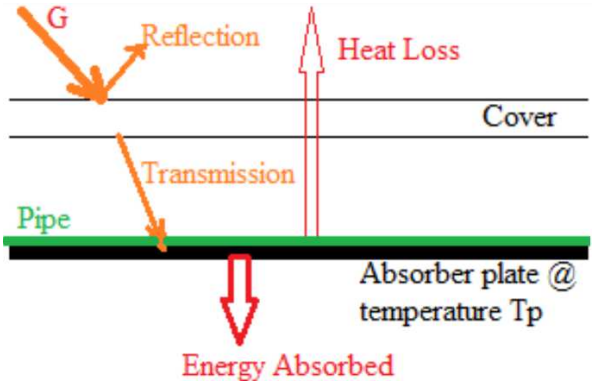

Fig. 3. Main parameters for heat transfer of the flat-plate collector.

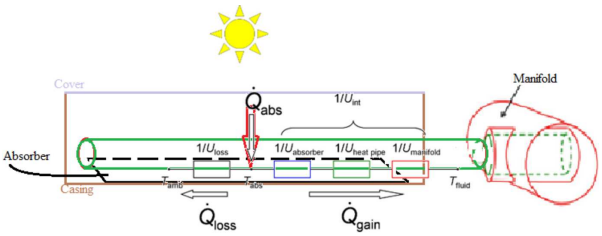

Fig. 4. Heat transfer and resistance network for the flat-plate collector.

In this study, the absorber plate has common standard characteristics to simplify the analysis. These are listed below [1, 3, 6, 7]:

- to absorb as much of the radiant energy of the Sun, as possible,
- to lose as little heat to the surroundings, as possible,
- to transfer the retained heat to a fluid.

The absorber plate carries out the energy conversion from solar radiation to internal energy of a fluid. The efficiency of a solar heating of a collector (absorbed energy/incident solar energy) depends on the difference in temperature between the absorber plate and its environment at each radiation level. For any given temperature difference, the efficiency is higher when solar radiation increases.

3. Materials and methods

Importance of efficient heat transfer in flat-plate collectors, where solar energy is converted into usable heat energy, has been ever increasing, with demanding solar energy applications. The efficiency typically decreases with the increase of temperature. Thus, the collector efficiency factor can be calculated by considering the temperature distribution of the absorber and by assuming that

the temperature gradient in the flow direction is negligible. From this point of view, we will start by writing heat transfer equations, which help to define the temperature gradient, for the first step of thermal analysis of the collector.

Generally, steady state heat conduction from the cover to the absorber is given by Eq. (1).

$$\nabla(k\nabla T) = 0. \tag{1}$$

The Fourier law of heat conduction describes the temperature distribution in any point in space or time. The partial differential equation of the Fourier law must be solved using known boundary conditions. If we consider a cylindrical geometry then for solid and liquid phase conditions of substance, the solution of uni-dimensional time-dependent heat transfer equation in cylindrical geometry is derived as time-dependent temperature distribution [8]. The basic quadratic equation is shown below for a one-dimensional plate, as considered in this study [5].

$$\frac{\partial T}{\partial t} - \alpha\frac{\partial^2 T}{\partial x^2} = 0. \tag{2}$$

From the simple thermal network, the heat loss due to forced convection on surfaces of a collector is given by Eq. (2). In other words, the sensible heat, transferred from absorber plate to the water is equal to that, which causes the temperature to rise, which can be written mathematically as Eq. (3) [4, 5, 9].

$$Q_{\text{loss}} = \frac{T_{\text{p}} - T_{\text{a}}}{R_{\text{L}}} = -U_{\text{L}}A(T_{\text{p}} - T_{\text{a}}), \tag{3}$$

where, T_{p} is absorber plate temperature, T_{a} is air (ambient) temperature, U_{L} is convective heat transfer coefficient, N_{p} is number of pipes, $R_{\text{L}} = 1/(U_{\text{L}}A)$, A is product of number of pipes N_{p}, diameter of pipe D_{p} and length of pipe L_{p}.

All three modes of heat transfer are involved, when considering a basic flat-plate collector. The conduction-convection equation is also solved for the heat transfer in the flowing water, which is shown in E. (4).

$$\rho C_{\text{pu}}\nabla T = \nabla(k\nabla T). \tag{4}$$

The longwave radiation heat loss can be calculated from Eq. (5).

$$q_{\text{lw}} = \varepsilon\sigma[(T_{\text{pv}})^4 - (T_{\text{amb}})^4]. \tag{5}$$

The water is heated in all designs by the absorber plate, transferring heat to the water, since heat transfer is driven by a temperature difference between two systems in thermal contact. All of above equations are prepared for the schematic diagram in Fig. 5, as the background to the thermal analysis.

Therefore, the question of what temperature difference drives heat transfer from the plate to the water, is answered in this study using the flat-plate collector of the Istanbul Technical University (ITU). The answer is the log mean temperature difference, as given by Eq. (6), which is derived by considering a differential energy balance between the water in thermal contact with the absorber [6, 7].

$$\Delta T_{\text{lm}} = \frac{[T_{\text{p}} - T_{\text{out}}] - [T_{\text{p}} - T_{\text{in}}]}{\ln\left(\frac{T_{\text{p}} - T_{\text{out}}}{T_{\text{p}} - T_{\text{in}}}\right)}, \tag{6}$$

where, T_{in} is entering water temperature, T_{out} is exiting water temperature and T_{p} is absorber plate temperature.

Now the rate of heat transfer from the absorber to water Q_{loss}, given by Eq. (3), becomes Eq. (7).

$$Q_{\text{loss}} = -U_{\text{L}}A\Delta T_{\text{lm}} = \dot{m}c_{\text{w,p}}\Delta T. \tag{7}$$

Negligible thermal resistance for the pipe wall itself is assumed, since most thermal resistance occurs between the water and the wall of the pipe.

Calculations are supported in this study by the thermal images. A clear, dry day was chosen for thermal image inspections. Solar radiation was measured using a solarymeter, to make sure that the solar radiation is above 650 W/m^2 [10]. The specifications of the real, working flat plate collector system, of the Istanbul Technical University are given in Table II.

TABLE II

Information of the system and location.

Location	Istanbul, TURKEY
Latitude	40°58′N
Longitude	28°50′E
Collector tilt	45°
Collector area	1.75 m^2
Collector type	Flat-plate
Collector cover number	Single
Storage tank type	Cylindrical
Tank volume	50 l

4. Results and discussion

The thermal analysis of the absorber was carried out in this study by considering a one-dimensional plate. This study is aimed to investigate the relations of temperature distribution in the absorber and the heat transfer from the absorber to the fluid, using heat transfer calculations, as mentioned above.

The operating point is found by simultaneously solving Eq. (7). Thus, the operating point was found to be $T_{\text{p}} =$ 32 °C (89.6°F) and $\Delta T =$ 12.88 °C (55.18°F). Operating point is shown in Fig. 5. Additionally, the experimental measured data of the case study are used to validate the numerical evaluation.

Heating of water in applications occurs well before this crossover temperature. This shows that a good solar engineering involves designing systems that can operate at the lowest possible temperature.

The operating point was also investigated using the thermal camera imagines and SmartView program (version 3.15 by Fluke Cop.). A Fluke Ti90 IR-thermograph camera was used for surface temperature measurements. Thermal imaging helps to identify heat loss, where high performing regions are impeded by lower performing regions and overheated connections. The IR gun looks for

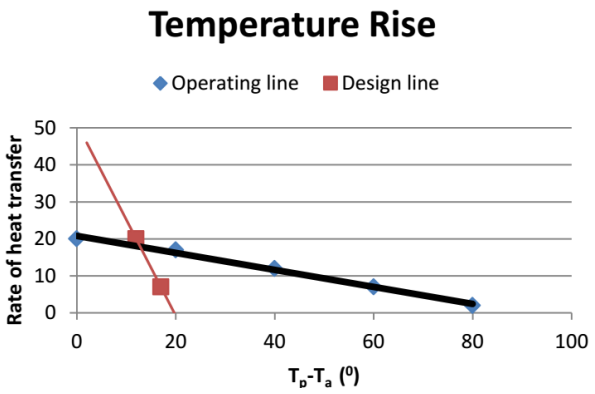

Fig. 5. Operating and design lines for the rise of hot water temperature in the flat plate collector, as functions of $T_\mathrm{p} - T_\mathrm{a}$.

the temperature of a relatively small spot (hotspots). Several readings were noted on collector, to obtain a more representative average surface temperature. The IR camera measures the emitted IR radiation from an object, because the emitted radiation is a function of the surface temperature of the object [11, 12]. The connection point in the image shows visible heating, as shown in Fig. 6.

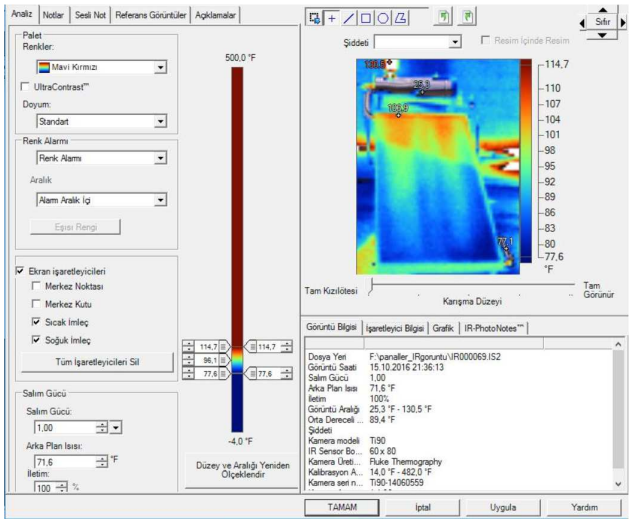

Fig. 6. The thermal image of glazing on the collector, with temperatures of individual defective part and analysis of the thermal image with Fluke-SmartView program.

Figure 6 shows IR image of flat-plate collector. The collector is built at Department of Physics Engineering in Maslak campus of ITU, Istanbul-Turkey [13]. The color of the image represents the intensity of the IR signal and temperature. The temperatures of defined regions of IR image are illustrated in Table III. By observing Fig. 6 with the temperature scale of 25.33–45.94 °C (77.6-114.7°F) and the rainbow scale, it can be said that the measured temperatures of every part of the collector fluctuate within the region of 30–32 °C (86–89.6°F). This small declination between calculated temperature and measured temperature can be considered normal, due to possible emissivity factor uncertainties and the fact that the collector is under no load.

Calibration range is between −10.0 °C (14°F) and 250.0 °C (482°F). Image range of the IR camera is between −3.7 °C(25.3°F) and 54.7 °C (130.5°F).

TABLE III

Backside temperature and minimum, maximum and average temperature values for defined four regions, such as hottest point, coldest point, region P_0 and region P_1.

Region point	Emisstivity power	Backside temp.	Min.	Aver.	Max.	Units
P_0	1	71.6	106.9	106.9	106.9	°F
P_1	1	71.6	77.1	77.1	77.1	°F
Hot	1	71.6	130.5	130.5	130.5	°F
Cold	1	71.6	25.3	25.3	25.3	°F

In the experimental part of this study it was observed, that if the solar radiation changes during the measurement, for example, due to clouding, the infrared image was unusable. For the best possible temperature differentiation it is recommended to carry out measurements when the outdoor temperatures are low. Therefore, the IR (thermal) image was taken at 16:00. It shows the temperature of the glazing on the collector.

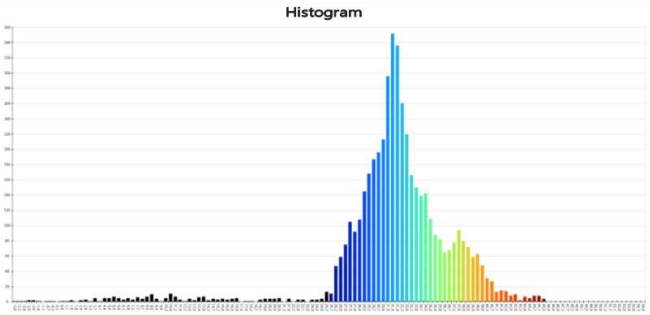

Fig. 7. The histogram graph of the thermal image of the inspected flat-plate collector (i.e.the temperature gradients of the glazing on the collector) on October 14th, at 16:00.

This is important because most of the collector heat loss occurs through the cover, and cooler cover is an indication of more efficient operation. The IR image in Fig. 7 shows a smooth increase in temperature from top to bottom. This is showing the actual temperature of the surface of the plate, which is proportional to the absorber temperature. The absorber temperatures seem to be on the high side, given that the transfer temperature was about 32 °C (89.6°F).

The acquired thermal images of the inspected flat-plate collector were analyzed in order to generate a simple and fast correlation between the thermodynamic model-based

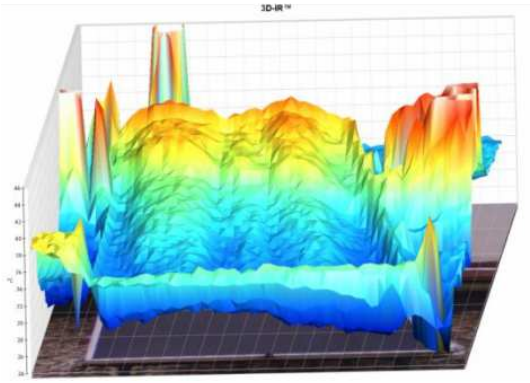

Fig. 8. The histogram graph of thermal image of the inspected flat-plate and three-dimensional temperature diagram of the collector (i.e. the temperature gradients of the glazing on the collector) on October 14th, at 16:00.

temperatures of the collector (estimated plate temperature, T_{p}) and the measured temperatures (measured surface temperature, T_{surface}), obtained from the in situ thermo-graphic inspection.

After analysis of Figs. 6–8, with the temperature scale (0–95 °C/32–203°F) and the color palette (rainbow scale), it can be said that the measured temperature T_{cm} values of each "healthy" solar collector of the module fluctuate within the region of 30–32 °C (86–89.6°F).

5. Conclusions

In this study heat transfer analysis of a flat plate collector has been considered. A considerable deviation from the literature has been made to incorporate engineering heat transfer calculations. An experimental study has been realized to investigate the pertinent correlation between the operating temperature of the absorber of a flat-plate collector in situ T_{surface}, measured using infrared thermal camera.

In conclusion, infrared thermograph appears to be a non-destructive method for the in situ evaluation of performance of a flat-plate collector. The method gives fast, quite reliable and easy to interpret results, regarding the condition of each part in a flat-plate collector. Unfortunately, specific limitations, related to emissivity problems, the presence of glass cover of the collector and the undesirable dependency from the environmental (ambient and background) conditions, have to be taken into account.

References

[1] M. Romero-Alvarez, E. Zarza, *Handbook of Energy Efficiency and Renewable Energy*, Chapt. 21, Concentrating Solar Thermal Power, Plataforma Solar de AlmeriaCIEMAT, Taylor & Francis Group, LLC, 2007.

[2] http://solarenergyforus.com/solar-thermal-system/.

[3] F. Struckmann, *Analysis of a Flat-plate Solar Collector, Project Report*, May 08, 2008 MVK160 Heat and Mass Transport, Lund, Sweden 2008.

[4] L. Ayompe, A. Duffy, *Appl. Thermal Engin.* **58**, 447 (2013).

[5] K.H. Kim, C. Ho Han, *Int. J. Mining Metallurgy Mechan. Engin. (IJMMME)* **2**, 2320 (2014).

[6] S. Chamoli, *J. Energy South. Africa* **24**, 8 (2013).

[7] B.M. Santos, M.R. Queiroz, T.P.F. Borges, *Brazilian J. Chem. Engin.* **22**, 277 (2005).

[8] M. Koru, O. Serçe, *Acta Phys. Pol. A* **130**, 453 (2016).

[9] Zhong Ge, Huitao Wang, Hua Wang, Songyuan Zhang, Xin Guan, *Entropy* **16**, 2549 (2014).

[10] J.L. Vásquez, S.T. Pérez, C.M. Travieso, J.B. Alonso, *Cognitive Computat.* **5**, 551 (2013).

[11] https://www.testequity.com/documents/pdf/Fluke-industrial-commercial-thermal-imagers-ds.pdf.

[12] http://en-us.fluke.com/products/infrared-cameras/fluke-ti90-infrared-camera.html.

[13] Z. Er, *Acta Phys. Pol. A* **128**, B-300 (2015).